SOUTHAMPTON OCEANOGRAPHY CENTRE

RESEARCH & CONSULTANCY REPORT No. 87

A wind tunnel study of the mean airflow around a simple representation of a merchant ship

**B I Moat[1], A F Molland[2]
and M J Yelland[1]**

2004

Report prepared for

Woods Hole Oceanographic Institution

[1]James Rennell Division for Ocean Circulation and Climate
Southampton Oceanography Centre
University of Southampton
Waterfront Campus
European Way
Southampton
Hants SO14 3ZH UK
Tel: +44 (0)23 8059 7739
Fax: +44 (0)23 8059 6204
Email: ben.moat@soc.soton.ac.uk

[2] University of Southampton, School of Engineering Sciences

DOCUMENT DATA SHEET

AUTHOR
MOAT, B I , MOLLAND, A F, & YELLAND, M J

PUBLICATION
DATE
2004

TITLE
A wind tunnel study of the mean airflow around a simple representation of a merchant ship.

REFERENCE
Southampton Oceanography Centre Research and Consultancy Report, No. 87, 21pp.
(Unpublished manuscript)

ABSTRACT

An investigation has been carried out to measure mean velocities above a solid block located in a wind tunnel. A Particle Image Velocimetry (PIV) system was used. The purpose of the investigation was to quantify the change in the mean flow speed caused by the bluff body and hence to determine the possible bias in wind speed measurement made from anemometers located above the superstructure of merchant ships. Possible sources of experimental error were investigated and resulted in; a) a blockage ratio correction which varied with position, b) the use of 2-dimensional maps of the free stream flow to obtain reference velocities and c) an estimate of a residual bias of up to 4% in the PIV wind speed data. The wind speed was accelerated by up to 28% compared to the free stream (or undistorted) wind speed. Close to the top of the block the wind speed is severely decelerated and the airflow reverses in direction. There was no dependence of either the pattern of the flow or of the magnitude of the wind speed bias on changes in wind directions of up to 30°.

KEYWORDS

airflow distortion,   bluff bodies,   merchant ship,   Particle Image Velocimetry,   PIV,   voluntary observing ships,   VOS,   wind speed error,   wind tunnel

ISSUING ORGANISATION

**Southampton Oceanography Centre
University of Southampton
Waterfront Campus
European Way
Southampton   SO14 3ZH
UK**

Not generally distributed - please refer to author

TABLE OF CONTENTS

NOTATION

H	Height of the block (m)
L	Length of the block (m)
B	Breadth of the block (m)
U	Nominal wind tunnel wind speed (ms^{-1})
ν_{air}	Kinematic viscosity of air at 15 °C (1.44×10^{-5} m^2s^{-1})
R_e	Reynolds number (based on block length) [$U.L/\nu_{air}$]
x	distance downstream from the upwind leading edge
z	height above the top of the block
x/H	normalised distance downwind of the upwind leading edge
z/H	normalised height above the top of the block
CFD	Computational Fluid Dynamics
COADS	Comprehensive Ocean Atmosphere Data Set
PIV	Particle Image Velocimetry
RANS	Reynolds Averaged Navier-Stokes
VOS	Voluntary Observing Ship
WMO	World Meteorological Organisation
YAG	Yttrium-Aluminum-Garnet

1. BACKGROUND

A large proportion of the merchant ship fleet is recruited by the World Meteorological Organisation's (WMO) Voluntary Observing Ship (VOS) programme to routinely report meteorological parameters at the ocean surface. These observations include: cloud type and cover, precipitation, air temperature, sea surface temperature, wind speed and direction and sea state. In general, merchant ships are large bluff body shapes and the air flow over the ship will be either accelerated or decelerated by the presence of the superstructure. This causes a bias in the wind speed measurements made from anemometers located on the ship and may have an impact on climate related studies which use these data. There is no knowledge of the sign or the magnitude of the possible biases in ship based wind speed measurements. Other studies have examined biases in VOS observations caused by the presence of the ship. For example, air temperatures measured by badly exposed instruments can be affected by heat from the ship and so data are biased high (Berry *et al.,* 2004); sea surface temperature data depend upon the measuring method used (Kent and Taylor, 2004). This paper examines the possible biases in VOS wind speed observations using results from a wind tunnel study of the air flow above a bluff body. This represents a first approximation of the flow above the bridge of a VOS ship. The experimental setup is described in Section 2 and the accuracy of the results is discussed in Section 3. The results of the experiments are presented and discussed in Section 4.

Experimental studies of the mean flow over bluff bodies are limited. Castro and Robbins (1977) measured the mean wind speed above and behind a surface mounted cube in a turbulent boundary layer flow. Martinuzzi and Tropea (1993) made measurements above a cube in a narrow channel and Minson *et al.* (1995) made measurements close to the top of a bluff body in a wind tunnel using a boundary layer flow. The study of Martinuzzi and Tropea (1993) was not applicable as it was a channel flow and the study of Minson *et al.* (1995) did not possess enough measurements in the region of interest. More importantly, the velocity profiles in all three cases were normalised by a reference wind speed obtained from a single location and are not representative of the free stream in the

5

region of interest.   In order to obtain the biases present in wind speed measurements from merchant ships, an absolute change in the mean wind speed from the free stream is required.   Therefore, the results presented in this paper are normalised by the free stream wind speed profile obtained at the region of interest, i.e. above the position of the block (with no block present).   This compensates for any variations in the free stream wind speed with position and height in the tunnel (Section 3.2).

2. EXPERIMENTAL SETUP

The low speed section of the University of Southampton 2.13 m by 1.52 m (7' by 5') wind tunnel, described by Davis (1961), was used to examine the flow over a bluff body.   The low speed section is 5 m long with a 4.6 m by 3.7 m working cross section.   A surface mounted solid block (Figure 1) of dimension 0.422 m (H), 0.294 m (L) and 0.595 m (B) was placed in the wind tunnel (Figure 2). The position of the ship model is also shown in Figure 2 and discussed in Section 3.1.   The wind tunnel was run at a nominal wind speed of 7 ms^{-1} which corresponded to a Reynolds number of 1.4×10^5 based on the block length.   The turbulent intensity of the wind tunnel between 1 Hz and 1 kHz was 0.2 % of the mean flow (Castro, 2002).

A Dantec Particle Image Velocimetry system (Dantec, 1988) was used to measure a grid of 2-dimensional velocities above the block.   A high power Neodymium-YAG (Nd:YAG) laser was mounted at a height of 1.97 m on a metal beam running the length of the tunnel working section.   The vertical laser sheet was orientated parallel to the mean flow direction, and a Dantec 80C60 Hi-sense digital camera was mounted in a metal frame 1.28 m from the measurement area. A smoke generator using regular smoke fluid was used to seed the airflow in the tunnel.   The vertical plane within the seeded flow was illuminated twice and the position of the seeded particles within the flow was recorded by the digital camera.   The time delay between illuminations was 0.5 μs.   The two images were stored and subdivided into 64 by 64 smaller areas, referred to as interrogation areas.   The particle displacements between each of the corresponding interrogation areas were determined using a cross correlation

technique (Dantec, 1988). A 2-dimensional velocity map was produced by dividing each particle displacement by the time delay between illuminations. The velocity maps presented in this paper were averaged from a sequence of 100 images recorded over a period of 50 seconds.

For flows normal to the block (i.e. a wind direction of 0°), four velocity maps were measured. These were combined (Figure 3) to produce a total of 73 (x, streamwise) by 59 (z, vertical) velocity measurements, with an area 0.36 m (x) by 0.29 m (z). As a check on the consistency of the PIV system, the camera was positioned so the four time averaged velocity maps overlapped by 0.03 m and 0.014 m in the streamwise and vertical directions respectively. For wind directions of 15° and 30° the block was rotated around the point where the centerline of the block intersects the upwind leading edge, i.e. x=z=0. Only one time averaged velocity map was measured in area 3 (Figure 3) for these two relative wind directions.

A portable thermal probe anemometer[1] (specified accuracy of 2 %) was used to investigate the changes in free stream wind speed at various locations (Figure 4) in the wind tunnel in the absence of the ship model (see Section 3.1). The results are shown in Figure 5 and highlight two main problems in determining what wind speed profile should be used to normalise the velocity measurements. Firsty, the mean free stream wind speed varied with position in the wind tunnel (Figure 5a) and differed by up to 1.5 ms^{-1} from its nominal set value of 7 ms^{-1}. Secondly, Figure 5 b shows that the mean wind speed measured in the same position could differ by the order of 0.5 ms^{-1} between the start and end of the experiment. The general shape of the wind speed profile showed that a wall jet was present close to the tunnel floor, although its effects were not significant at the top of the block (z=0.422 m). These variations in the nominal tunnel wind speed caused problems when trying to normalise the wind speeds obtained around the block geometry. Therefore, to quantify the absolute wind speed errors, the block was periodically removed and PIV velocity maps of the free stream

[1] Airflow Developments Ltd., TA-5 Thermal anemometers, High Wycombe, Buckinghamshire, HP12 3QP. UK.

velocities were obtained at each of the four areas above the block.   These free stream velocities were used to normalise the wind speed measurements made in the same location but with the block present, and hence obtain the absolute wind speed biases.   All wind speed profiles presented in this paper have been normalised in this manner.

3. EXPERIMENTAL ACCURACY

3.1 Corrections applied to the PIV measurements

No standard blockage correction was applied to the measurements as the maximum blockage ratio (frontal area of the block : area of the wind tunnel section) during the experiment was 1.6 %.   This ratio is less than the typical values recommended by Barlow *et al*. (1999) and corresponds to that used in Castro and Robins (1977).

This experiment was the first in a series of experiments.   Later experiments modelled the flow over two blocks in order to better represent the shape of VOS ships.   The block in this study represented the deck house block of a VOS ship and it was necessary to locate it close to the wind tunnel contraction (Figure 2) in order to leave room for the two block models (Figure 4).   It was thought that the contraction may affect the air flow above the block so a Computational Fluid Dynamics (CFD) study of the airflow through the wind tunnel was performed.

The CFD code used was the commercial Reynolds Averaged Navier-Stokes (RANS) code VECTIS (Ricardo, 2001).   The RNG $k \sim \varepsilon$ turbulence closure scheme was used for all simulations.   The CFD simulations in this paper were isothermal, i.e. the air, the block sides and the wind tunnel walls were set at a constant temperature of 20°C.   For bluff body flows Moat (2003) performed a sensitivity study of VECTIS to determine the dependence of the solution on the mesh density, the turbulence closure scheme and the shape of the upstream wind speed profile.   The findings of Moat (2003) were applied to the CFD studies of the airflow in the wind tunnel and resulted in an effectively mesh independent solution with variations in wind speed of 4 % or less.

A CFD simulation of the 3-dimensional airflow over the block in the wind tunnel with the contraction (Figure 6) was compared to a similar simulation with no contraction (Figure 7). The wind speed profiles above the block were normalised by free stream wind speed profiles determined by repeating the two CFD simulations with the block removed. Figure 8 shows the normalised wind speed profiles from the wind tunnel models with and without the contraction. The CFD simulation with the contraction showed an increase of up to 8 % in the normalised wind speed, when compared to the simulation with no contraction. It is already known that the block gives a blockage ratio of 1.6 % which, in the absence of the contraction, does not have a big effect since the flow is only accelerated by 1.6 % across the whole cross section of the tunnel. When the tunnel contraction is introduced the 1.6 % blockage ratio results in a flow that is accelerated by 8 % in the lower part of the tunnel (above the deck house block), and shows negligible acceleration towards the roof and walls. It is thought that the contraction was concentrating the acceleration of the flow towards the centre of the lower part of the tunnel. Correction profiles were calculated from the ratio of the normalised wind speed profiles from the with-and-without contraction CFD simulations and applied to the PIV measurements presented in this paper.

3.2 Consistency of the PIV measurements

Webb and Castro (2003) observed differences of up to 10 % in wind speed measurements made using the Dantec PIV system compared to standard measurement methods. This discrepancy was not located in the region of accelerated flow but within a recirculation bubble. Nevertheless, it highlights that wind tunnel measurements using PIV could be prone to measurement errors. These errors could be due to the shape of the boundary layer profile, changes in velocity in the wind tunnel, and the set up of the PIV system. This section examines the wind tunnel data to determine the magnitude of any systematic errors in the wind speed results.

The PIV velocity maps were overlapped to determine any bias in the measurements. The time delay between the measurements varied from 1 hour to

1 day.   Even with the long delay between measurements, a comparison of the overlapping regions suggested that changes in the wind speed measurements were generally 4 % or less.   This was confirmed by obtaining two velocity maps at the same location 1 day apart, which showed a consistent bias of 3 % over the whole area.

A possible cause of the 4 % systematic error may be the variation of the free stream wind speed in the tunnel with time (as shown in Figure 5b).   Throughout the experiments the wind tunnel was run at a variable dynamic pressure (constant fan speed) to try and maintain an approximately constant wind speed.   In order to determine the variation in the wind speed using this method, the free stream wind speed was measured 13 times over a period of 3 hours at a location that corresponded to 'area 3' (Figure 3) with no block present.   Time series of the mean wind speed at a height of 0.5 m above the tunnel floor and of the wind tunnel temperature are shown in Figure 9.   In Figure 9 the error bars indicate the standard error.   Within a period of 40 minutes, variations in free stream wind speed of up to 0.2 ms^{-1} were observed.   There was no obvious relationship to variation in temperature.

In summary, it can be concluded that the PIV wind speed measurements examined here are accurate to within 4 %.

4. WIND TUNNEL RESULTS

This section examines the biases in the wind speed measurements made above a bluff body.   The dependence of the normalised wind speed profiles with changes in wind direction and with distance from the upwind leading edge is discussed.   The vertical profiles of the normalised wind speed at relative wind directions of 0°, 15° and 30°,   and at distances of x/H=0 to x/H=0.3 are shown in Figure 10.   For distances greater than x/H=0.3 the normalised wind speed profiles for a flow normal to the block (0°) are shown in Figure 11.   In order to compare these with later results, all distances are scaled by the block height, H.   In both figures, the vertical dashed line indicates normalised wind speeds of 1.0 where the measured speed equals the free stream speed.

Above the upwind leading edge of the bridge (Figure 10a) the wind speeds are accelerated by 10 % to 18 % compared to the free stream and do not vary a great deal with height compared with those further downwind. Further aft (Figures 10b to d) the wind speed is severely decelerated close to the top of the bridge, and then increases with height to a point where it is equal to the free stream flow, i.e. a normalised wind speed of 1.0. Above the decelerated region the normalised wind speed increases rapidly to a maximum of about 1.2 (at x/H=0.1) to 1.28 (x/H>0.3), i.e. the flow was accelerated by up to 28 % compared to the free stream value. It is expected that the wind speed will decrease further towards the free stream value with increasing height, although this was not measured.

Apart from at the upwind leading edge there is a region of air flowing counter to the wind direction (normalised wind speed <0) within the decelerated region (Figure 10b to d). The counter flow of air close to the top of the block is greater at a relative wind direction of 30° (Figures 10c, d). This is due to air flowing up the rear face of the block (Figure 3) and entering the decelerated region at larger angles of incidence. At all three relative wind directions there was no evidence of any reattachment of the flow to the top of the block. Apart from the region of counter flow close to the top of the block, it is clear that there is no dependence in either the general pattern of the flow or the magnitude of the wind speed maximum with relative wind direction.

At distances greater than x/H=0.3 and for a flow normal to the block the magnitude of the counter flow increases with distance from the upwind leading edge (Figure 11). Similarly, the positions at which the wind speed equals the free stream flow (normalised wind speed of 1.0), and the position of the wind speed maximum increase in height with distance from the upwind leading edge. In contrast to Figure 10, the magnitude the wind speed maximum does not vary significantly with distance from the upwind leading edge and was approximately constant (normalised wind speed of 1.27).

Wind speed measurements on ships can be made more accurately by locating anemometers in regions where the spatial gradient in airflow distortion is

small and the bias introduced is well defined.   The normalised wind speed field above the block is shown in Figure 12.   Close to the line where the measured wind speed equals the free stream wind speed (normalised wind speed of 1.0) the normalised wind speed varies rapidly between 0.2 and 1.35.   Such large gradients suggest that positions along this line are not ideal locations for anemometers.   To reduce the effect of airflow distortion on wind speed measurements made above bluff bodies it is apparent that anemometers should be placed as close as possible to the upwind leading edge and as high as possible above the top of the block.

5. CONCLUSIONS

1)   The wind tunnel results provide an understanding of the biases that may be present in anemometer wind speed measurements made above the bridge of merchant ships.   Prior to these results, neither the sign or magnitude of the biases were known.

2)   The investigations showed that at all distances back from the upwind leading edge the wind speed was severely decelerated close to the top of the block.   Within the decelerated region the air was recirculated with a flow counter to the wind direction.   Above the counter flow region the wind speed increased with height to a point where it equalled the free stream flow, i.e. a normalised wind speed of 1.0.   Above this height the wind speed was accelerated rapidly to a maximum of 20 % to 28 % above the free stream wind speed and then decreased with increase in height.

3)   There was no significant dependence in either the pattern of the flow or in the magnitude of the wind speed with relative wind directions of 0°, 15° and 30°.

4)   It is recommended that anemometers located above bluff bodies are positioned as close as possible to the upwind leading edge and as high as possible above the top of the body.

5) The results provide data suitable for validation of the flow over bluff bodies.

REFERENCES

Barlow J. B., W. H. Rae and A. Pope, 1999: Low speed wind tunnel testing (3rd edition), John Wiley and Sons, USA. 713 pp.

Berry, D. I., E. C. Kent and P. K. Taylor, 2004: An analytical model of heating errors in marine air temperatures from ships. *Journal of Atmospheric and Oceanic Technology*. (accepted)

Castro I. P. and A. G. Robins, 1977: The flow around a surface-mounted cube in uniform and turbulent streams, *Journal of Fluid Mechanics*, **79**, 307-335.

Castro I. P., 2002: Personal communication, Southampton University, UK.

Dantec, 1988: Flowmap Particle Image Velocimetry Instrumentation. Dantec Measurement Technology A/S, Tonsbakken 18, DK-2740 Skovlunde, Denmark. [Available from Dantec Dynamics Ltd. Bristol. UK.]

Davies P. O. A. L., 1961: The new 7×5 ft. and 15×12 ft low speed wind tunnel at the University of Southampton. A.S.S.U Report Number No. 202. University of Southampton, UK,

Kent, E. C. and P. K. Taylor, 2004: Towards Estimating Climatic Trends in SST, Part 1: Methods of Measurement. *Journal of Atmospheric and Oceanic Technology*. (submitted)

Martinuzzi R., and C. Tropea, 1993: The flow around surface-mounted, prismatic obstacles placed in a fully developed channel flow, *Journal of Fluids Engineering*, **115**, 85-92.

Minson A. J., C. J. Wood, and R. E. Belcher, 1995: Experimental velocity measurements for CFD validation, *Journal of Wind Engineering and Industrial Aerodynamics*, **58**, 205-215.

Moat B. I., 2003: Quantifying the effects of airflow distortion on anemometer wind speed measurements from merchant ships. PhD. Thesis, School of Engineering Sciences, University of Southampton, UK. 163 pp.

Ricardo, 2001: VECTIS Computational Fluid Dynamics (Release 3.5) users guide, Ricardo Consulting Engineers Ltd., Shoreham-by-Sea, United Kingdom, 262 pp.

Webb S. and I. P. Castro, 2003: PIV, LDA and HWA comparative measurements in various turbulent flows, Technical Report AFM-03/1, Aerodynamics and Flight Mechanics Research Group, University of Southampton, UK. 23 pp.

FIGURES
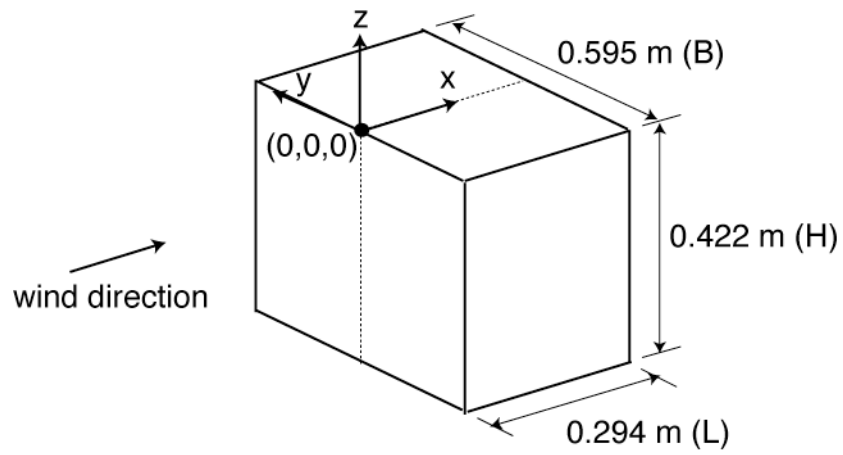
Figure 1   The dimensions of the block and the co-ordinate system used.
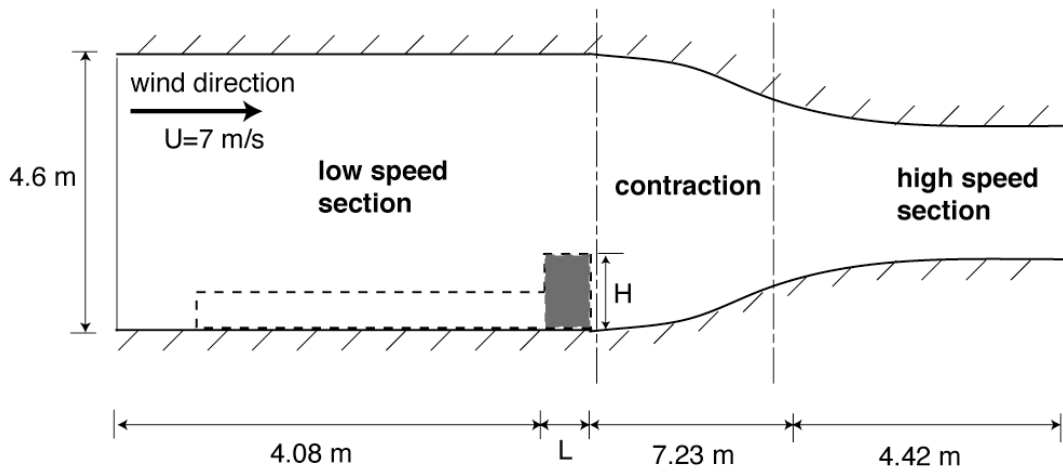
Figure 2   A schematic showing the position of the block (shaded rectangle) and
ship model (dashed outline) in the wind tunnel.
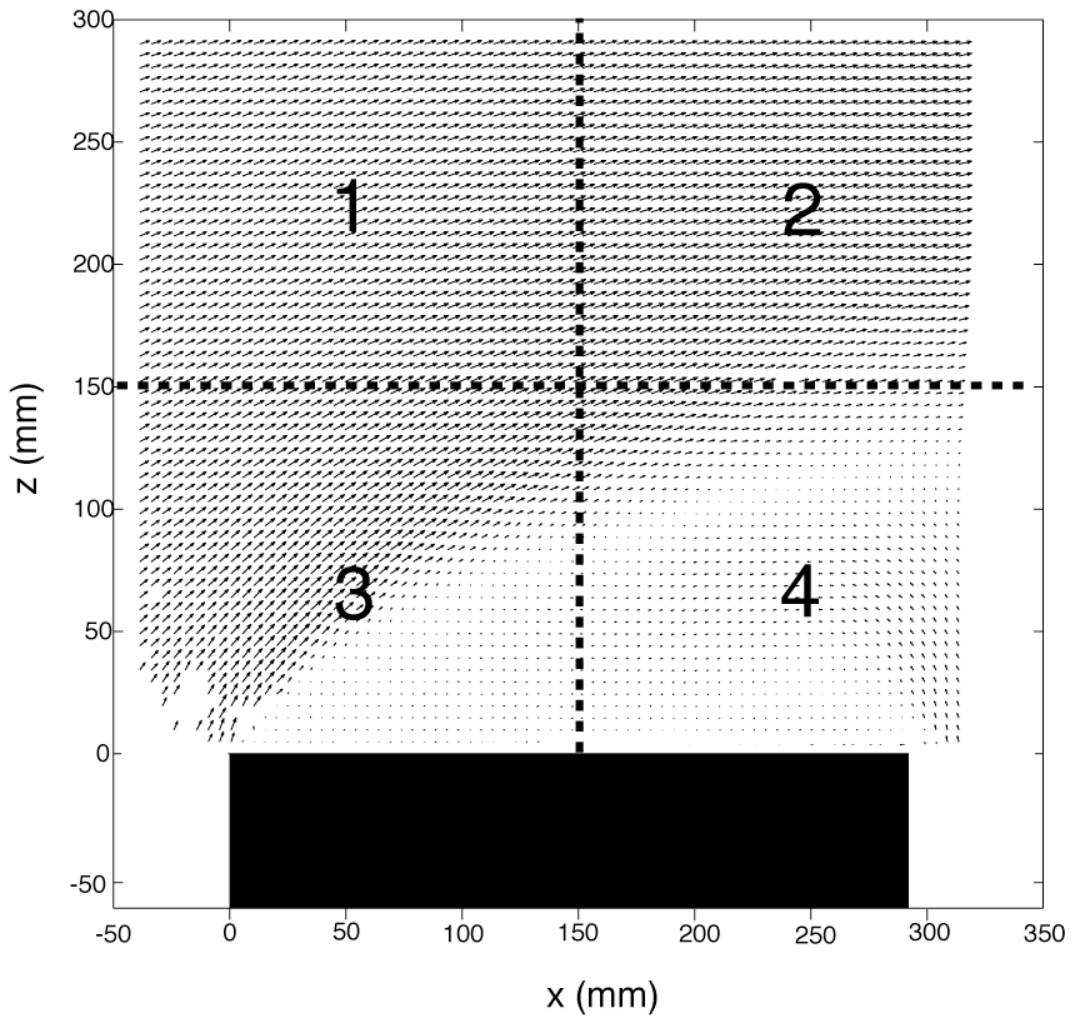
Figure 3   PIV measured velocities along the centreline for a flow normal (0°) to the block.   The dashed lines indicate the four velocity maps.   The free stream flow is from left to right.
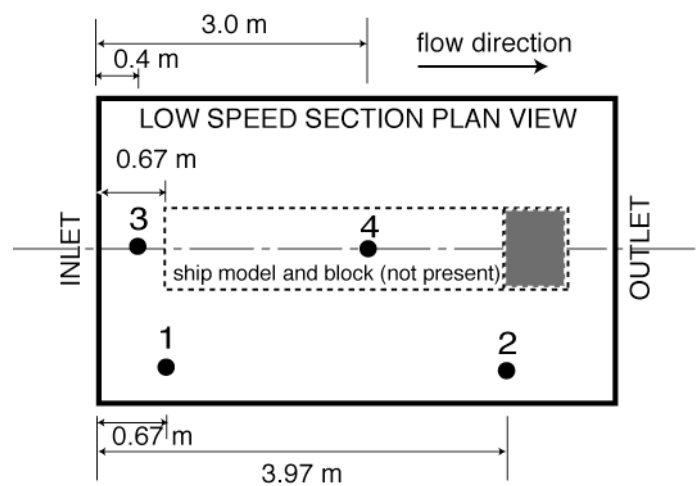

Figure 4   Plan view showing the thermal probe measurement locations in the wind tunnel.   The position of the ship model (dashed outline) and the block (shaded rectangle) are shown.

16
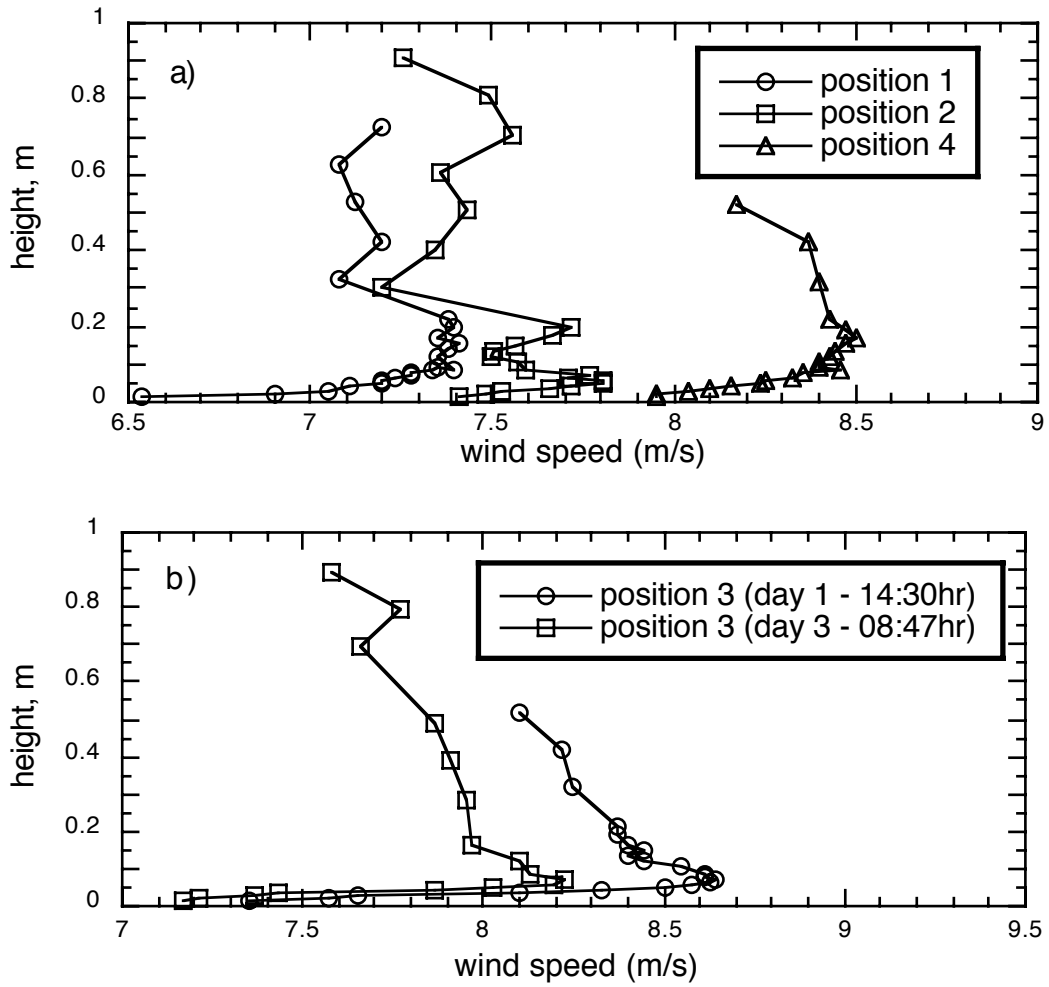
Figure 5   The vertical profiles of the free stream wind speed at the positions
shown in Figure 4.
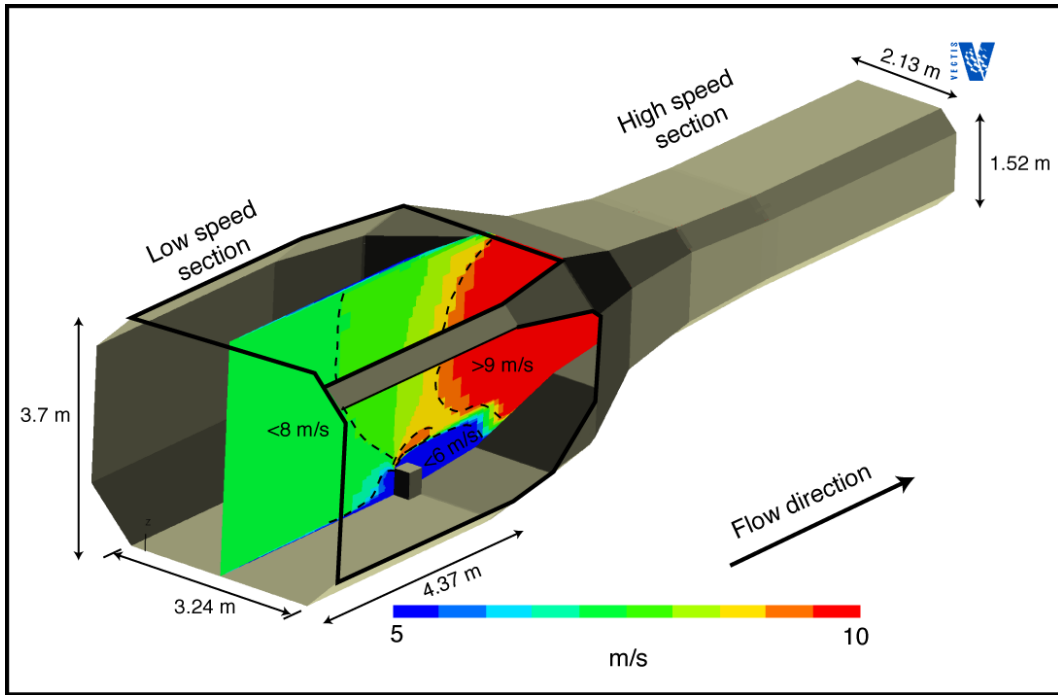
Figure 6   The CFD simulation of the airflow through the University of
Southampton wind tunnel.   The velocity field in the centre of the tunnel
is displayed.
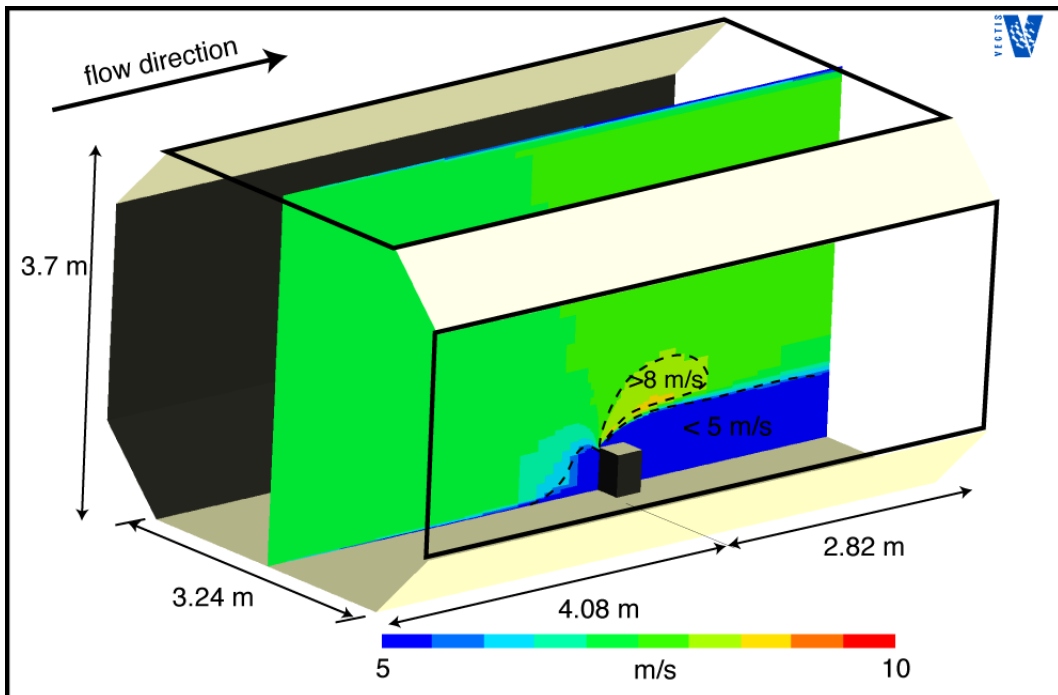
Figure 7   The CFD simulation of the airflow over the block, enclosed in the low
speed section of the wind tunnel.   The velocity field in the centre of the
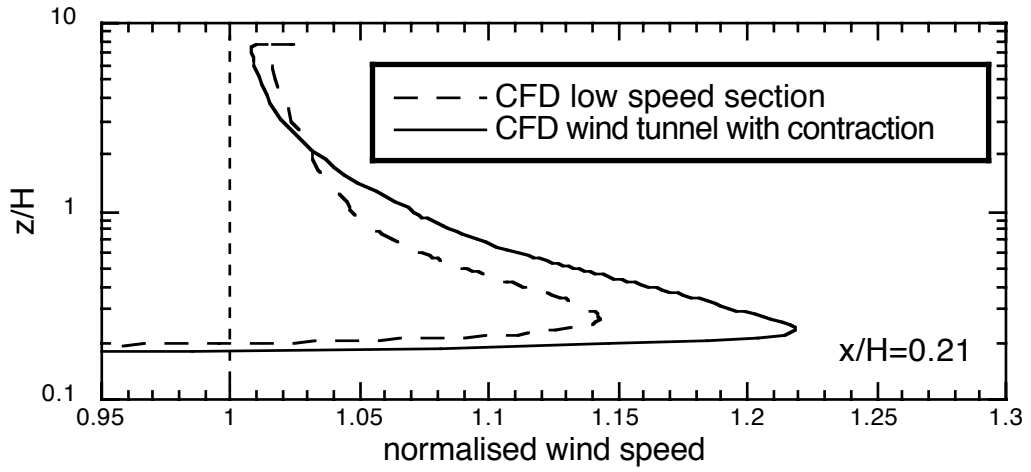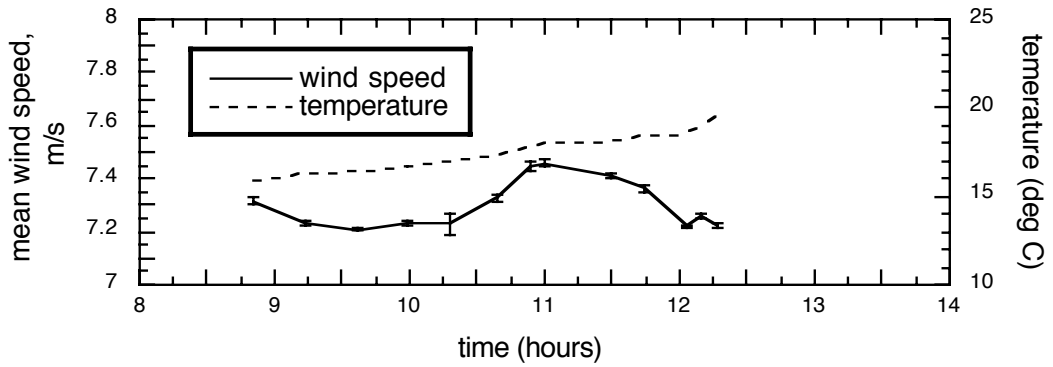tunnel is displayed.

Figure 8   CFD simulations of the normalised wind speed profiles above the block.

Figure 9   Time series of the mean free stream wind tunnel speed and temperature
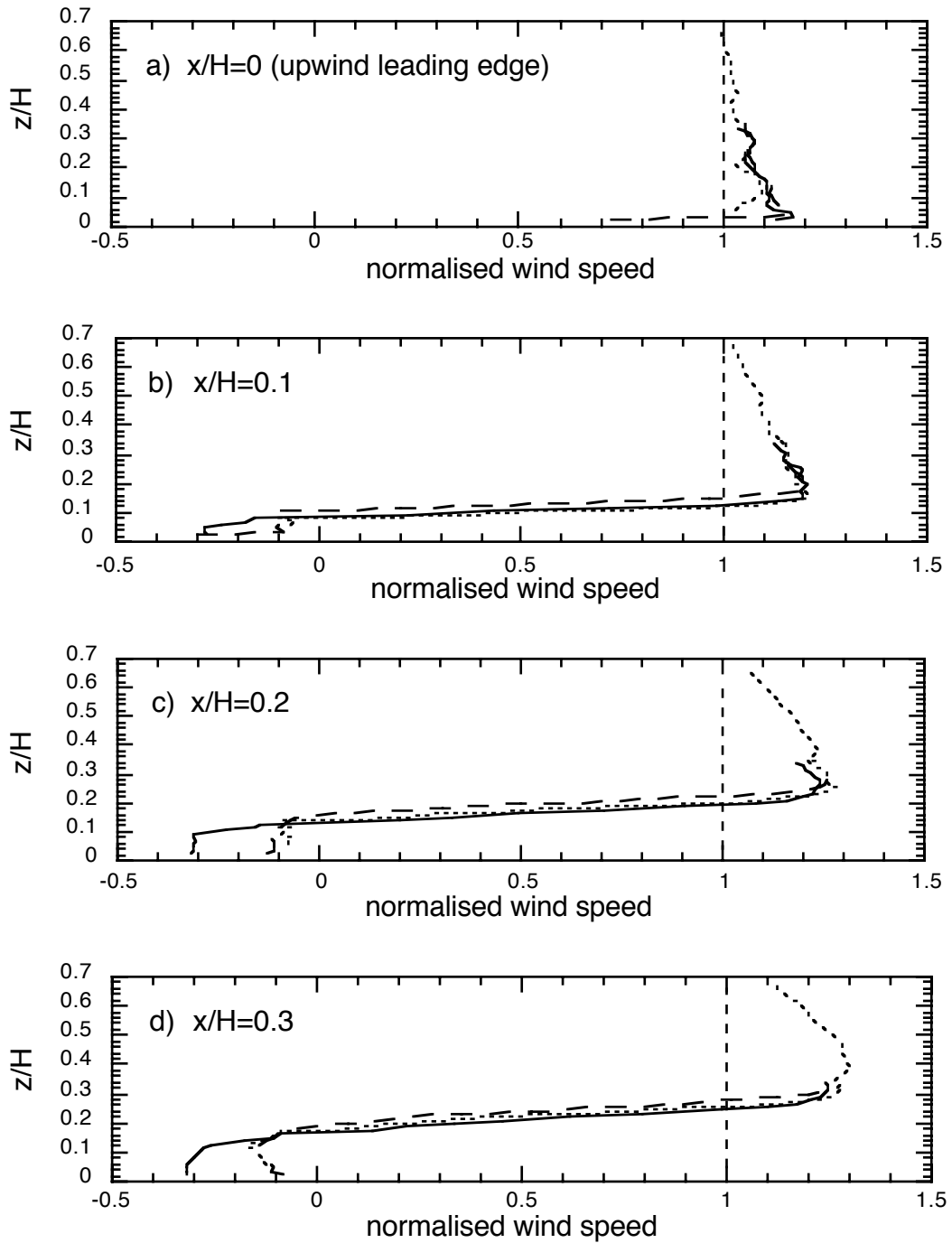with the wind tunnel run with a constant fan speed.

Figure 10   Normalised PIV wind speed profiles above the block for flows normal

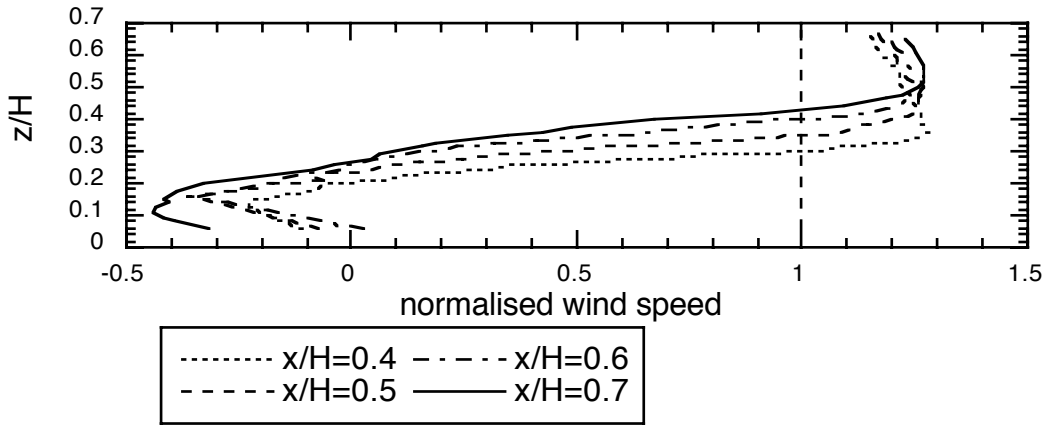to the block 0 ° (short dashed line), 15° (long dashed line) and 30°

(solid line).

Figure 11   Normalised PIV wind speed profiles above the block for a flow normal to the block (0 °).
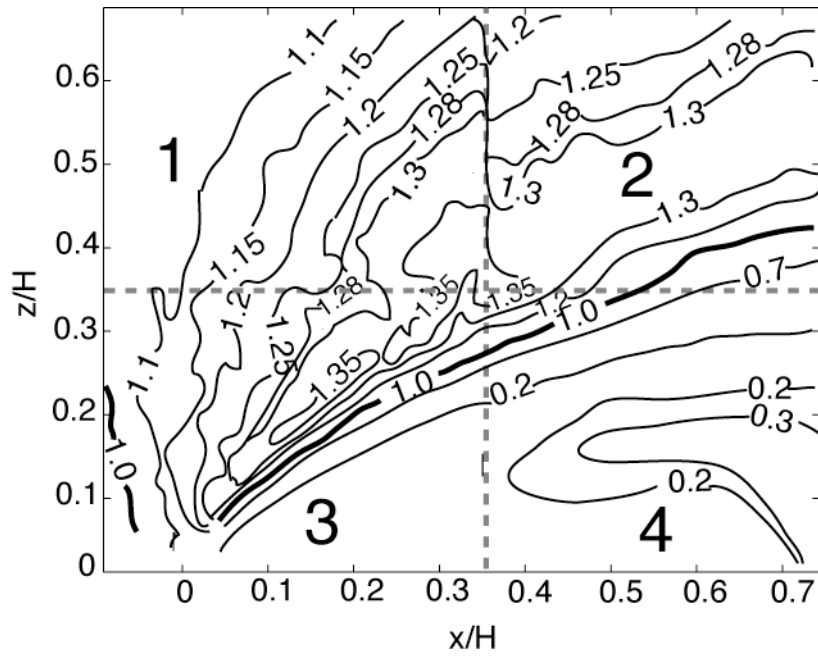
Figure 12   PIV normalised wind speed along the centreline of the block, for a flow normal (0°) to the block.